Earth and Planetary Science Letters, 109 (1992) 319–332
Elsevier Science Publishers B.V., Amsterdam

[MK]

Tectonic context of fluid venting at the toe of the eastern Nankai accretionary prism: Evidence for a shallow detachment fault

N. Chamot-Rooke [a], S.J. Lallemant [a], X. Le Pichon [a], P. Henry [a], M. Sibuet [b], J. Boulègue [c], J.-P. Foucher [d], T. Furuta [e], T. Gamo [e], G. Glaçon [f], K. Kobayashi [e], S. Kuramoto [e], Y. Ogawa [g], P. Schultheiss [h], J. Segawa [e], A. Takeuchi [i], P. Tarits [j] and H. Tokuyama [e]

[a] *CNRS URA 1316, Laboratoire de Géologie, Ecole Normale Supérieure, 24 rue Lhomond, 75231 Paris Cedex 05, France*
[b] *Département Environnement Profond, IFREMER-Centre de Brest, B.P. 70, 29263 Plouzané, France*
[c] *Laboratoire de Géochimie et Métallogénie, T.16-26, E.5, Université Pierre et Marie Curie, 4 place Jussieu, 75252 Paris Cedex 05, France*
[d] *Département Géosciences Marines, IFREMER-Centre de Brest, B.P. 70, 29263 Plouzané, France*
[e] *Ocean Research Institute, University of Tokyo, Minamidai 1-15-1, Tokyo 164, Japan*
[f] *CNRS UA 1208, Laboratoire de Dynamique des Plate-formes carbonatées, Centre de Sédimentologie-Paléontologie, Université de Provence, 3 place Victor Hugo, 13331 Marseille, France*
[g] *Department of Earth and Planetary Sciences, Kyushu University 33, Fukuoka 812, Japan*
[h] *Schultheiss Geotek, Marley Lane, Haslemere, Surrey GU27 3RF, UK*
[i] *Department of Geology, Toyama University, Toyama 930, Japan*
[j] *Institut de Physique du Globe, 4 place Jussieu, 75252 Paris Cedex 05, France*

Received May 27, 1991; revision accepted December 16, 1991

ABSTRACT

During the Kaiko-Nankai diving cruise the peak of the venting activity was located near the top of the very first anticline. The most prominent morphological feature between the mid-slope (3870 m) and the apex of the fold (3770 m) is a 20 m high cliff cutting through subhorizontal massive mudstones affected by numerous joints. The trend of this scarp is oblique to the fold axis and structurally controlled along two sharply defined NNE–SSE and E–W directions. Fresh talus and blocks found locally suggest active tectonics and recent erosion. Intense deformation is evident from strongly tilted strata restricted to the base of the cliff that we interpret as an upslope thrust. At the scale of Seabeam mapping, this thrust can be followed eastward for more than 5 km along the 3820 m isobath. Two seismic lines recorded during one of the pre-site surveys show deformation at shallow depth, including small-scale folding and thrusting affecting only the wedge-shaped top sequence. Deeper layers can be traced continuously below this sequence. We conclude that the boundary between the "piggy-back" basin and the frontal fold turbidites acts as a shallow detachment fault, and interpret the base of the cliff as the outcrop of the fault. Dense colonies of *Calyptogena* clams and strongly nonlinear thermal gradients locate the major peak of fluid activity at the edge of the plateau above the main cliff. Scattered biological colonies as well as white bacterial mats and cemented chimneys were also found in a narrow belt along the base of the cliff. Fluid activity is thus closely related to the shallow detachment fault, fluid being expelled both at the outcrop of the fault and above it through the overlying strata, possibly using the very dense joint network.

1. Introduction

Long-distance migrations of fluids in accretionary complexes were first evident from deep-sea drilling results, and as a major result of ODP Leg 110, thermogenic methane was found in the interstitial waters from the décollement and the frontal faults at the toe of the Barbados accretionary prism [1]. This methane cannot be produced *in-situ* but rather comes from the deeper part of the prism, at least a few tens of kilometres landward. A consistent hydrogeological interpretation is that in the Barbados prism, fluids from a deep origin flow along the décollement and the three frontal thrusts [1–3] and propagate seaward, feeding a diapiric field [4–6]. The submersible exploration of the Barbados [6,7], Ore-

Correspondence to: N. Chamot-Rooke, CNRS URA 1316, Laboratoire de Géologie, Ecole Normale Supérieure, 24 rue Lhomond, 75231 Paris Cedex 05, France.

gon [8–10] and Nankai [11–15] trenches provided evidence from the seafloor of methane-rich fluid outflow, biological communities, bacterial mats, carbonate concretions and cemented chimneys. During the first eastern Nankai accretionary prism submersible survey, the main biological colonies based on chemosynthetic processes had been found above the frontal thrust [11]. Conversely, on the Oregon margin, the outcrop of the frontal thrust is not always associated with fluid seeping systems [9], suggesting that erosion and clogging are important in determining the spatial distribution of the vents with respect to the fault outcrops.

A major breakthough in fluid venting studies was to investigate the flow rates in a quantitative way, using either thermal constraints [16–23] or chemical constraints and direct measurements [24]. Fluid budgets indicate that the fluid output is about two orders of magnitude greater than the amount expected from steady-state compactional dewatering [20–22,25], pointing to large recharge at deep (flow along the décollement) or shallow (local recharge) levels, or to non-steady-state output. To properly estimate both fluid output (fluxes) and fluid path (geometry of the conduits), one needs a complete description of the surface manifestations and a correlation of these with tectonic features. Tectonics may increase the permeability of rocks through fracturing within faults. This would tend to channel flow along major faults and along the décollement. Tectonics may also increase the vertical permeability through dense jointing, particularly near the apex of folds. In the absence of tectonics, on the other hand, permeability is controlled by lithology and cementation. Flows would tend to occur along high-permeability sedimentary layers, especially if outflow is possible along erosional features.

We report here on a dense submersible survey over an active venting site of the eastern Nankai accretionary prism. The main objective is to map both the surface manifestations of fluid venting and the tectonic features in order to propose a fluid path model for the area.

2. Structural framework

The preliminary deep-tow camera site survey across the accretionary prism discovered two sites of active fluid venting [26]. The shallow site (2000 m deep) is located in the older part of the prism [27] and is closely related to a major backthrust over a slope basin [28]. We focus our attention on the deepest site (3800 m, hereafter site 1) located near the apex of the frontal fold (Fig. 1). The site 1 area is characterized by a low-angle tapered wedge resulting from the recent seaward propagation of a series of thrusts within the turbiditic trench fill. The result is the formation of a broad unit, bounded to the south by the frontal thrust (T1a −4020 m) and to the north by a major scarp (T2a −3500 m), which is the continuation of the east Tenryu basal thrust system. In its western part, this recent unit is about 7 km wide, at the location where the thrusts abruptly terminate into a complex lateral ramp system trending N310°E, roughly parallel to the local convergence motion between the Philippine Sea plate and the Eurasia plate. The unit widens progressively eastwards, reaching more than 10 km at its eastern end and finally vanishes east of 138°E. The total strain thus gradually decreases eastwards. The unit itself can be subdivided into two main subunits, each about 5 km wide (Fig. 1). The inner (landward) unit is a broad curved 400 m high anticline, thrust over the outer (seaward) unit along thrust T1b. A typical piggy-back basin develops on its back, apparently undeformed. The deformation of the outer unit is not homogeneous. To the west, the outer unit consists in a complex series of small anticlines and related thrusts, the overall structure being thrust over the trench fill along a single frontal thrust. To the east, the internal deformation pattern changes from small-scale folds and thrusts to a very flat and broad anticline as the total strain decreases. Changes do not seem to occur gradually but rather abruptly across transverse structures. East of 137°57′ the frontal thrust splits into a set of two high-angle thrusts 1 km apart (T1a and T1a', see Fig. 1). At the same location, the proto-thrust zone is well expressed as an elongate fold seaward of the main trench channel.

3. Microbathymetry of the venting site area

Two-thirds of the outer unit were explored in the course of fourteen dives, starting from the trench. Fluid venting manifestations were found to be confined to a very narrow zone near the top of the frontal fold. Although the frontal thrust is very active west of site 1 in the Tenryu Canyon area, as shown during the first Kaiko project [11,16], no fluid venting activity was found at the outcrop of the frontal thrust (T1a) in the site 1 area. The dives thus focused on the active site at depths ranging from 3840 m to 3770 m. A particularly dense coverage was obtained in a 1000 m^2 box close to the apex of the frontal anticline. The great number of dives there allowed us to map in detail the topographic and tectonic features in the venting system area. The bathymetry was obtained by adding the pressure gauge immersion of the submersible to the sonic altitude above the seafloor. The microbathymetric map shown in Fig. 2 uses these submersible depths combined with the acoustic navigation of the *Nautile*.

The microbathymetric map reveals the existence of an important cliff where strata outcrop. This is about 20–30 m high between 3830 and 3800 m. Although the main trend of the cliff is roughly E–W, the detailed mapping shows three segments (shaded area in Fig. 2), one trending N120°E (west of 137°54.35′), a central one trending N40°E and an eastermost one trending N110°E (east of 137°54.45′). These regular trends suggest that the cliff is structurally controlled. Above the cliff, the flat-topped, very first fold has a N70°E trending axis. From 3830 m to 3860 m, a small bench lies between the upper cliff and the main lower steep slope. We show below that the cliff between 3830 and 3800 m is the most active tectonic feature along the section and that fluid activity is focused in this area.

4. Geological observations by submersible

At the base of the section (Fig. 3; 4040 m), the outcrop of the frontal thrust (T1a), as defined from seismic data, was found to be covered by a sedimentary apron composed of very soft mud.

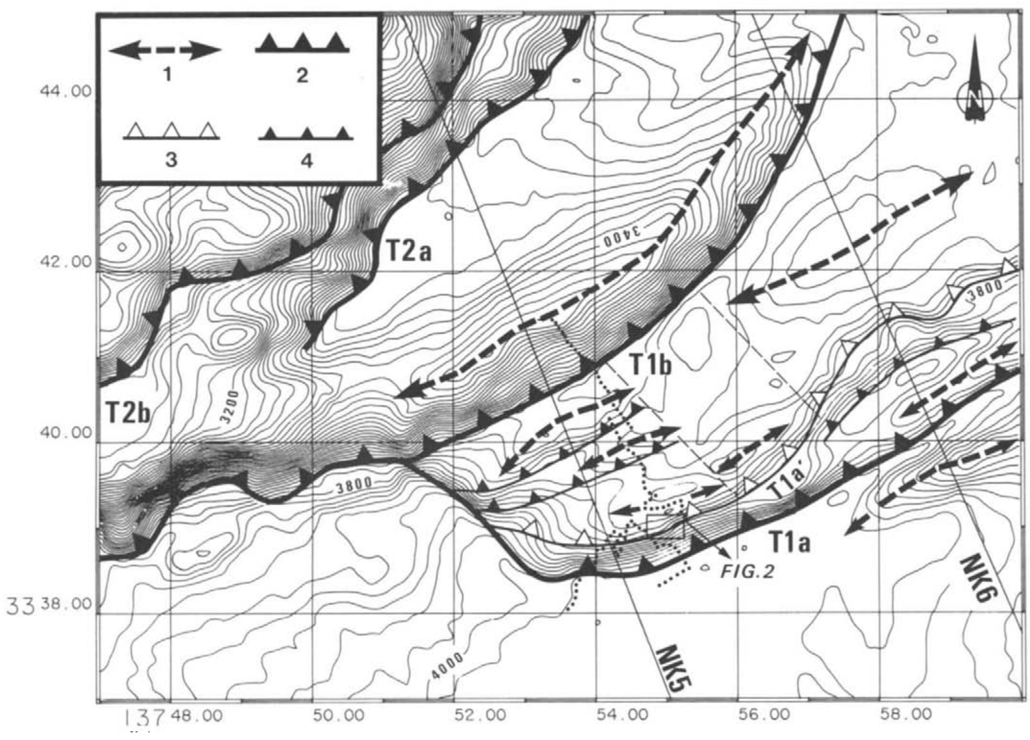

Fig. 1. Seabeam (isobaths every 20 m) and structural map of the Kaiko-Nankai area. Seabeam data were acquired by the Ocean Research Institute (University of Tokyo) aboard the *Hakuho-Maru* (cruise KH-89-1) as a pre-site survey for the Kaiko-Nankai cruise. The small box locates venting site 1. Additional dives outside the box are shown as dotted lines. *1* = Fold axis; *2* = main thrusts; *3* = shallow detachment fault; *4* = minor thrusts. The tracks of seismic lines NK5 and NK6 across the outer unit are also shown. The major thrusts discussed in the text are named T1a, T1b, T2a and T2b.

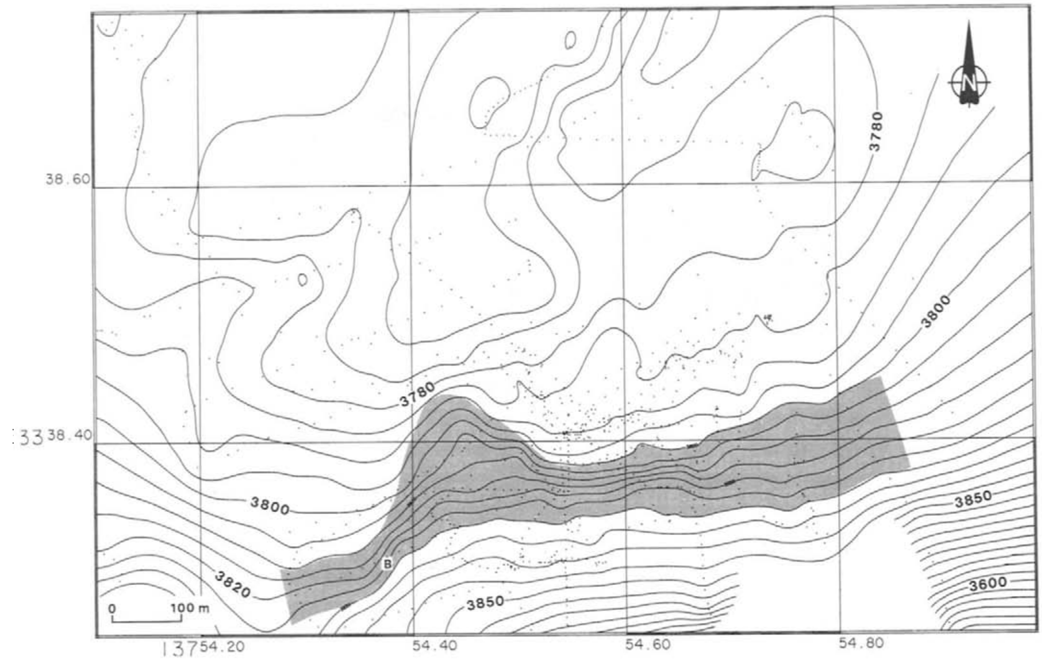

Fig. 2. Microbathymetry of the venting site (contour interval 5 m) and data points used for the interpolation. The main cliff is shaded. The upper edge of the cliff corresponds to the outcrop limit observed from submersible. The lower limit follows the 3830 m isobath. Letter *B* refers to the bottom photograph shown in Fig. 4B.

As already mentioned, no fluid activity was found there. The absence of fluid activity along the frontal thrust was confirmed during two other dives located 1 km east and 3 km west of the section. The deepest erratic blocks of mudstones appear at a depth of 3970 m. Stratified mudstones then outcrop at a depth of 3950 m, dipping downslope (10–20°) and conformable to the slope. Strata then progressively increase in dip (30°) and become successively parallel (3930 m) and slightly steeper (3900 m) than the slope. Although the rocks sampled are mostly mudstones, we did observe at 3930 m well-graded siltstones and mudstones, which we interpret as turbidites. Typical turbiditic sequences were also observed 3 km west of this section during Dive 17 at the 3890 m

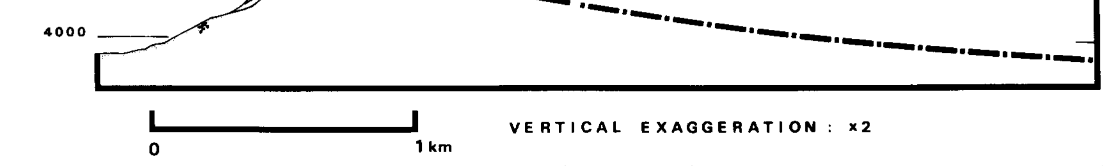

Fig. 3. Summary structural section of the outer unit along Dive 1 (X. Le Pichon) based on submersible observations. Triangles are clam colonies. The thick dashed line follows the proposed shallow detachment fault.

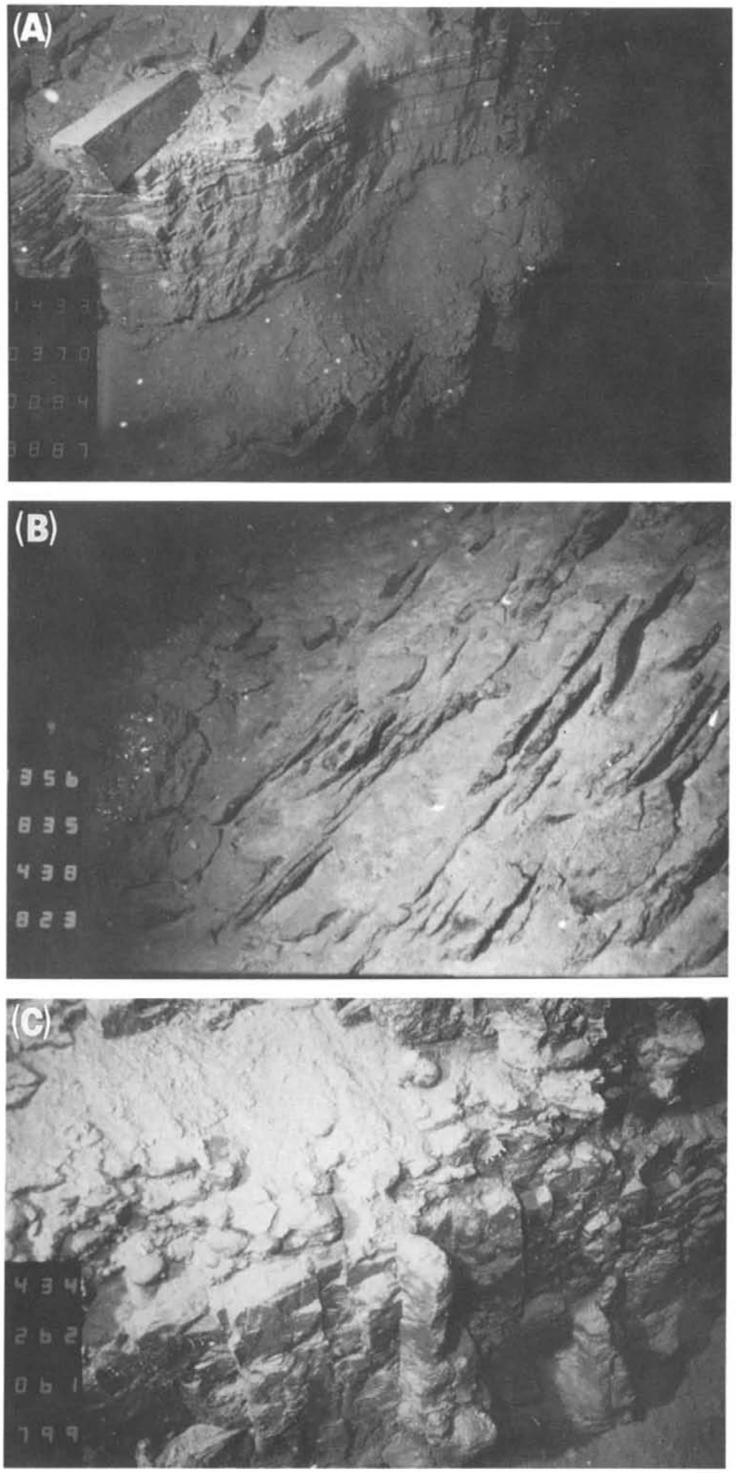

Fig. 4. Bottom photographs: (A) Turbiditic sequence including a small whitish ash layer, cut by orthogonal joints (Dive 17, N. Chamot-Rooke, 3887 m). (B) Tilted strata at the base of the cliff (Dive 23, M. Sibuet, 3823 m). (C) Abrupt scarp in the massive mudstones of the cliff (Dive 20, P. Henry, 3799 m).

depth (Fig. 4A). Sampling and dating of these turbidites gave a late Quaternary age (< 0.23 Ma, nannozone NN21). The outcropping sedimentary sequence is thus fairly young, possibly younger than 0.3 Ma. Consequently, the sedimentary sequence appears to have been deposited in the trough and later uplifted to form the scarp. Conglomeratic layers were ubiquitously found interbedded with stratified mudstones. The size of the conglomerate clasts ranges from pebbles (several centimetres) to blocks of about 1 m in size. A conglomeratic layer was sampled during

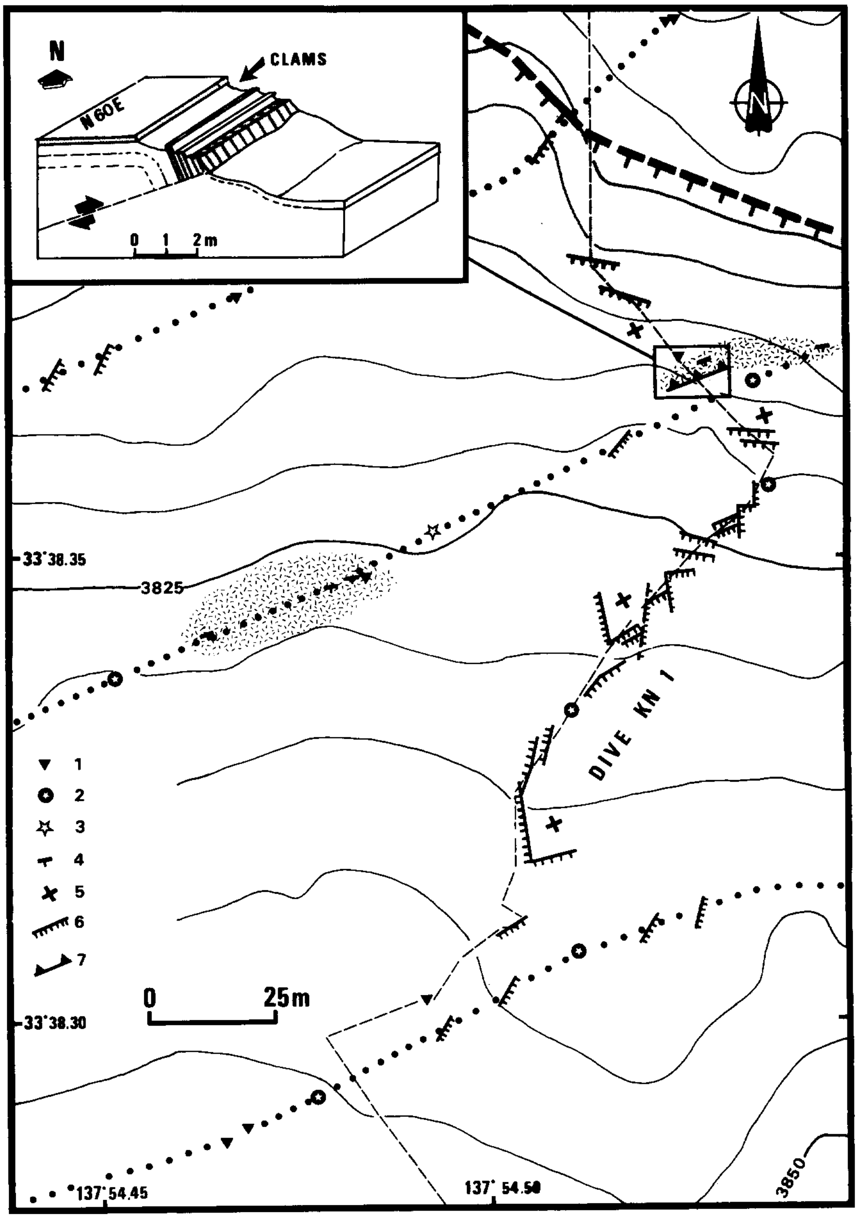

Fig. 5. Detailed structural sketch map in the vicinity of the upslope cliff, based on a N–S portion of Dive 1 and three E–W portions of Dive 23. *1* = Clam colonies; *2* = white patches; *3* = chimney; *4* = tilted strata; *5* = subhorizontal strata; *6* = minor scarps; *7* = thrust. The areas where strata are strongly tilted are shaded with ticks. The main cliff is shaded grey.

Dive 3 (1 km east of Dive 1) at a depth of 3965 m and was dated as late Pliocene based on the nannofossils present. No foraminifera were observed. During Dive 17, a Pleistocene age of 1.1–1.3 Ma was found for a mudstone sample collected at a depth of 3923 m, 30 m below the well-identified late Quaternary turbiditic sequence described above. Here again, nannofossils are rare and foraminifera are absent. Both samples are best interpreted as containing reworked fossils.

The first (deepest) clam field was discovered on a small bench at a depth of 3845 m (Fig. 3). Figure 5 is a structural sketch of this area. Subhorizontal strata were followed along a small promontory oriented N70°E up to a depth of 3820 m at the base of the cliff. The pile of thin, layered, subhorizontal strata is affected by numerous orthogonal joints (E–W and N–S), each individual stratum being sharply cut along these preferentially oriented trends, leading to a typical serrated fabric. Fields of large clams and white mats of probable bacterial origin were also found there.

The base of the cliff is marked by a drastic change in the strata attitude at a depth of 3820 m, the strata dipping to the south more steeply than the slope and reaching dips of 50–60° (Fig. 4B and 5). In the cliff, the sedimentary sequence consists of more massive mudstones in thick layers cut by numerous joints that are spaced more widely than in the sequence below (Fig. 4C). The steeply dipping layers, which are found in several places at the base of the cliff, have a consistent N80°E trend (Fig. 5). Furthermore, the tilted layers are alternations of thin siltstone and mudstone layers, similar to the sequences found in the bench between the depths of 3850 and 3820 m, and are clearly not the thick mudstone layers of the cliff. We thus favour a tectonic origin for the systematic tilting of the strata at the base of the cliff.

The top of the hill forms a broad bulge culminating at a depth of 3770 m without obvious outcrops, although the morphology suggests the existence of a N70°E-trending anticline. Further north, we successively cross two small south-facing cliffs immediately following small featureless depressions. Each of them shows downslope-dipping mudstone layers. On the basis of the seismic data (discussed in section 6), we interpret these two cliffs as the outcrops of secondary thrusts and folds (Fig. 2 and 3).

We conclude that the most deformed and the most active zone of the whole section is located at the base of the upslope cliff at the 3820 m depth. We show below that the major fluid venting manifestations are found in the vicinity of this upslope cliff.

5. Tectonics and venting activity

Numerous fluid seeps have been discovered in this area. These seeps were easily identified because of their association with chemosynthetic-based biological communities (bivalves and tube worms) or with white patches attributed to bacterial mats and to carbonate deposition features, including venting chimneys. Their activity was evaluated through thermal gradient measurements [22,23] and geochemical measurements [29–30, see also 21].

Four types of biological communities have been defined based on the characteristics of the community (density and species composition) [22]. Here, we only consider the distribution of type A colonies, which are large colonies (up to 2 m in diameter) composed mostly of small- and medium-sized clams (genus *Calyptogena*) with a few large ones. Their density is very high, up to 1000 individuals/m^2, and the sediments display evidence of strong bioturbation. Thermal measurements (down to 50 cm below the seafloor) are in good agreement with vertical advection at Darcian velocities of the order of 150 m a^{-1} (5.10^{-6} m s^{-1}) [22]. We also consider the distribution of the whitish bacterial mats, which are characterized by a very high content of hydrogen sulphide, a reduced salinity and calcium carbonate saturation [J. Boulègue, pers. commun., 1990]. On the basis of limited thermal measurements, Henry et al. [22] propose that these mats occur over relatively slow seeps (10 m a^{-1}, or 3.10^{-7} m s^{-1}). The chemical and thermal results are interpreted as indicating high dilution with seawater for the type A seeps and much smaller dilution for the bacterial mat seeps.

We summarize in Fig. 6 the fluid venting information (bacterial mats, type A colonies, and venting chimney) and the tectonic observations (scarps

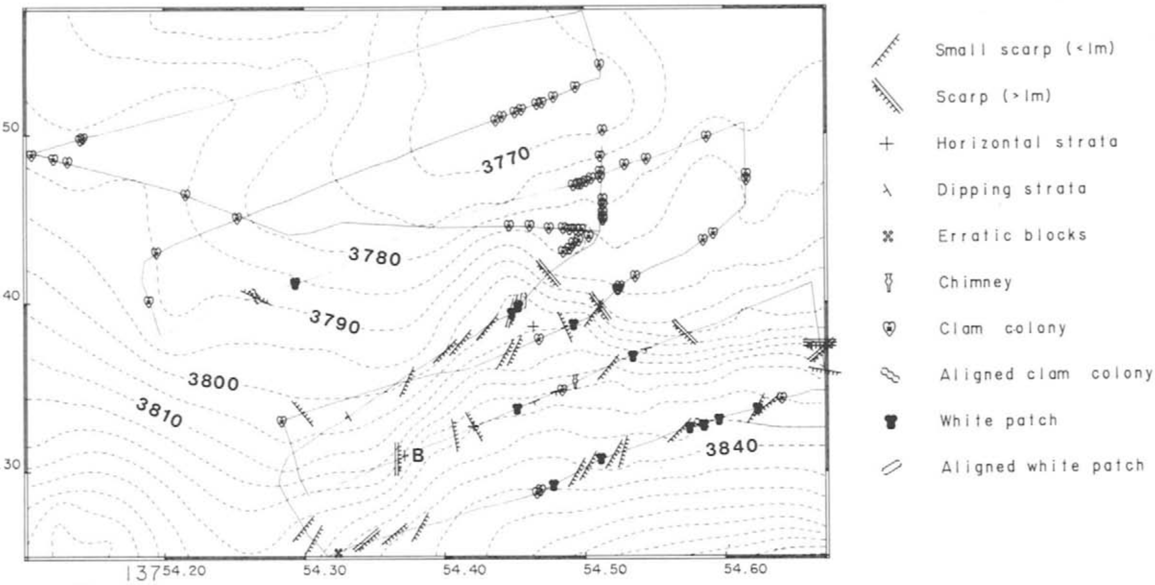

Fig. 6. Dive 23 observations (M. Sibuet) in the vicinity of the cliff, showing the relationship between the tectonic features and the fluid venting manifestations. Letter *B* refers to the bottom photograph shown in Fig. 4B.

and bedding attitude) from Dive 23, which was devoted to a regular systematic survey (grid-like tracks and constant speed). The two main types of seeps (type A colonies and the bacterial mats referred to as "white patches") occur in two completely different settings, with little overlap. Type A colonies are numerous above 3800 m on the top of the broad fold, beyond the upper edge of the cliff. Conversely, bacterial mats are almost exclusively situated on the bench at the base of the cliff between 3850 and 3820 m. White patches are frequently found in the vicinity of sedimentary layer outcrops. Aligned white patches were found mostly parallel to the local trend of the "scarplets", pointing to venting along strata. However, at some places, they crosscut the scarps. White patches were also sytematically found at the base of the major scarps along the N110°E segment. Most of the type A colonies were found in undisturbed areas, away from sedimentary outcrops.

6. Bathymetric and seismic reflection evidence for a shallow detachment fault

The tectonic features and fluid seepage distribution discussed above are best interpreted in terms of a thrust outcropping near the base of the cliff along which fluids circulate. The bathymetric map of Fig. 1 shows that the bench at the foot of the scarp near 3820 m widens significantly eastwards and then narrows again. Immediately east of the surveyed area, the upslope cliff becomes well defined even at the Seabeam scale (20 m contour interval). In addition, the upslope cliff trace is not parallel to the trace of the frontal thrust but has a broad curved outline roughly following the isobaths, as expected for a flat fault.

Fig. 7a displays a six-channel reflection profile (NK5, see location in Fig. 2) shot by the Ocean Research Institute of Tokyo University as a presite survey for the Kaiko-Nankai diving cruise. Although the resolution is poor, continuous planar reflectors dipping gently towards the north can be traced below the mostly unresolved nearsurface wedge-shaped structure. Profile NK6 (Fig. 7c, see location in Fig. 2), which is further east, indicates the presence of a flat planar reflector outcropping at the level of the bench. Above this reflector, the sequence appears discordant and slightly folded. Depth-converted line drawings of those two profiles are shown in Fig. 7b (NK5) and 7d (NK6).

The surface trace of the thrust and bathymetric and seismic reflection evidence are best interpreted as resulting from slight folding (NK6) or

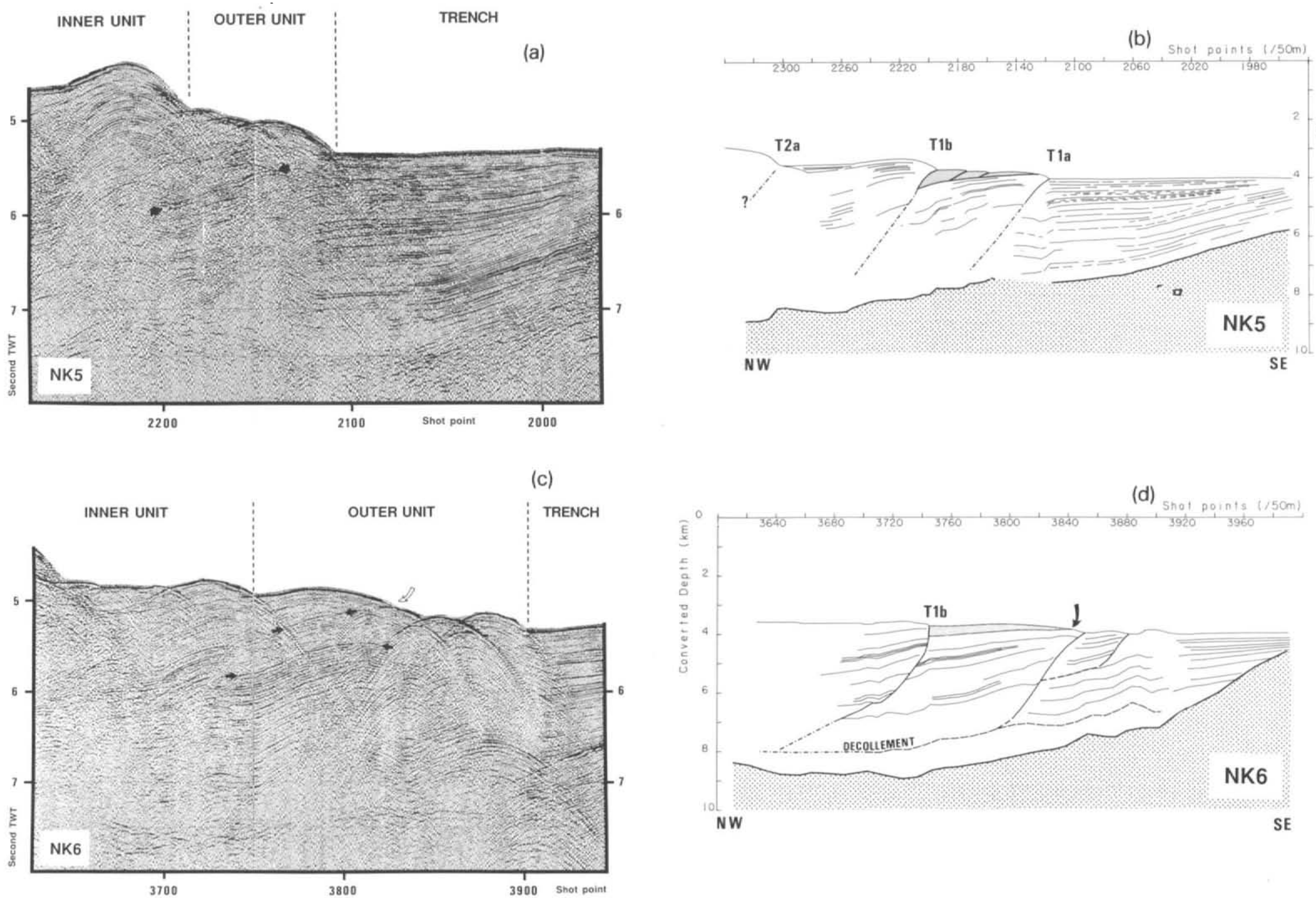

Fig. 7. Multichannel seismic lines NK5 and NK6 shot by the Ocean Research Institute as a site pre-site survey for the Kaiko-Nankai cruise (see location in Fig. 1). In (a) and (c) black arrows pinpoint a series of continuous reflectors below a near-surface fold and thrust system. The open arrows points to the bench at the base of the cliff. Depth-converted line drawings from a part of seismic lines NK5 and NK6 are shown in (b) and (d), summarizing our interpretation in terms of a "piggy-back" basin scraped off above a shallow detachment fault located at the boundary between the turbidites and the piggy-back basin sequence. The arrow marks the outcrop of the detachment fault.

thrusting and folding (NK5) of a sedimentary sequence above a shallow reverse detachment zone parallel to the underlying strata. The wedge shape of the overlying sequence cannot be a simple consequence of the deformation above the detachment fault, the total shortening and thus thickening being rather small. This sequence might have been deposited in a piggy-back basin, like that which still exists further east where the deformation of the outer unit disappears. Active piggy-back basin formation in the area is evident further north in the inner unit, between thrusts T1b and T2a (see map in Fig. 1 and line drawing in Fig. 7b). The proposed shallow detachment fault was then probably located at the base of the piggy-back basin sequence, along or near the lithological boundary. This is in good agreement with the submersible observations, as the sediments observed are more clayey in the upper cliff than in and below the bench. Note that the higher clay content would decrease the permeability and might help to explain the channeling of the fluid along the detachment fault. We thus interpret the venting site as the outcrop of a shallow detachment fault. In the following section, we show that at a smaller scale (diving observations), the outcrop of the fault is in fact a complex zone involving deformation of the underlying strata.

7. Tectonic interpretation of the shallow detachment fault outcrop

The main cliff shows a well-defined inverted V-shape, due to the intersection of the N40°E and N110°E segments located at 137°54.45′ (Fig. 2). The linearity of the two scarps attests to their tectonic origin. The seeps appear to be concentrated, for the type A colonies as well as for the bacterial mats, near the V-shape area (Fig. 6). The base of the main scarp is the boundary between the upper massive mudstones and the lower layered strata. It is also a site of active fluid seepage, as white patches were systematically found along it on the N110°E segment (see section 5). A striking observation is that the strongly tilted strata near the 3820 m water depth define a narrow N70°E-trending belt oblique to the two segments. However, this trend is exactly parallel to the fold axis above the cliff. Furthermore, the fold has a maximum amplitude in front of this narrow belt. We propose relating both structures to shortening above and within a complex detachment zone possibly located below a major lithological boundary. In other words, at the scale of the diving observations the detachment is a zone of a few tens of metres in thickness rather than a single flat thrust.

To illustrate this idea, we constructed a balanced cross section using the fault-bend fold theory [31] based on topographic and geological information (Fig. 8, see Fig. 3 for the location of this figure). The upper section (Fig. 8a) shows the sedimentary layer outcrops, the observed bedding attitude and the occurrence of the two types of seeps (A type colonies and white patches), in relation to the proposed detachment fault. In the interpreted section that we propose in Fig. 8b, we consider that the narrow belt of dipping layers constitutes the forelimb of a fault-bend fold. The thickness of the thrust packet is defined by the location of the boundary between the massive mudstones and the underlying turbidite-like sequences. We then construct a second ramp-and-flat system in order to account for the fold affecting the upper massive mudstones. Although we are aware of the non-uniqueness of the solution, it is satisfactory for obtaining a self-consistent section which fits the near-bottom observations. The most interesting result of this approach is that any realistic geological interpretation should involve a relatively thick (25 m) zone of duplex-type deformation below the main lithological boundary between the layered trench-fill sequences and the massive piggy-back basin sequence.

8. Fluid paths

The lower section in Fig. 8c is a tentative interpretation of the fluid paths. The simplest interpretation is that fluid is migrating along the previously defined fault detachment zone. This interpretation is in good agreement with the geochemistry of the fluids sampled during the dives [29,30], fluids seeping at the emergence of the detachment fault being less diluted (i.e. with lower chlorininity and higher content of hydrogen sulphide, and a very high methane content [29]) than the fluids expelled above the cliff. Based on thermal modeling, Henry et al. [22] have shown that downwelling of seawater occurs around the A type colonies located above the cliff. They show also that this type of local free-convection may be driven by a salinity difference as small as few permil between the deeper upcoming fluid and the seawater. We propose that low-chlorinity and methane-rich fluids that originated at depth mi-

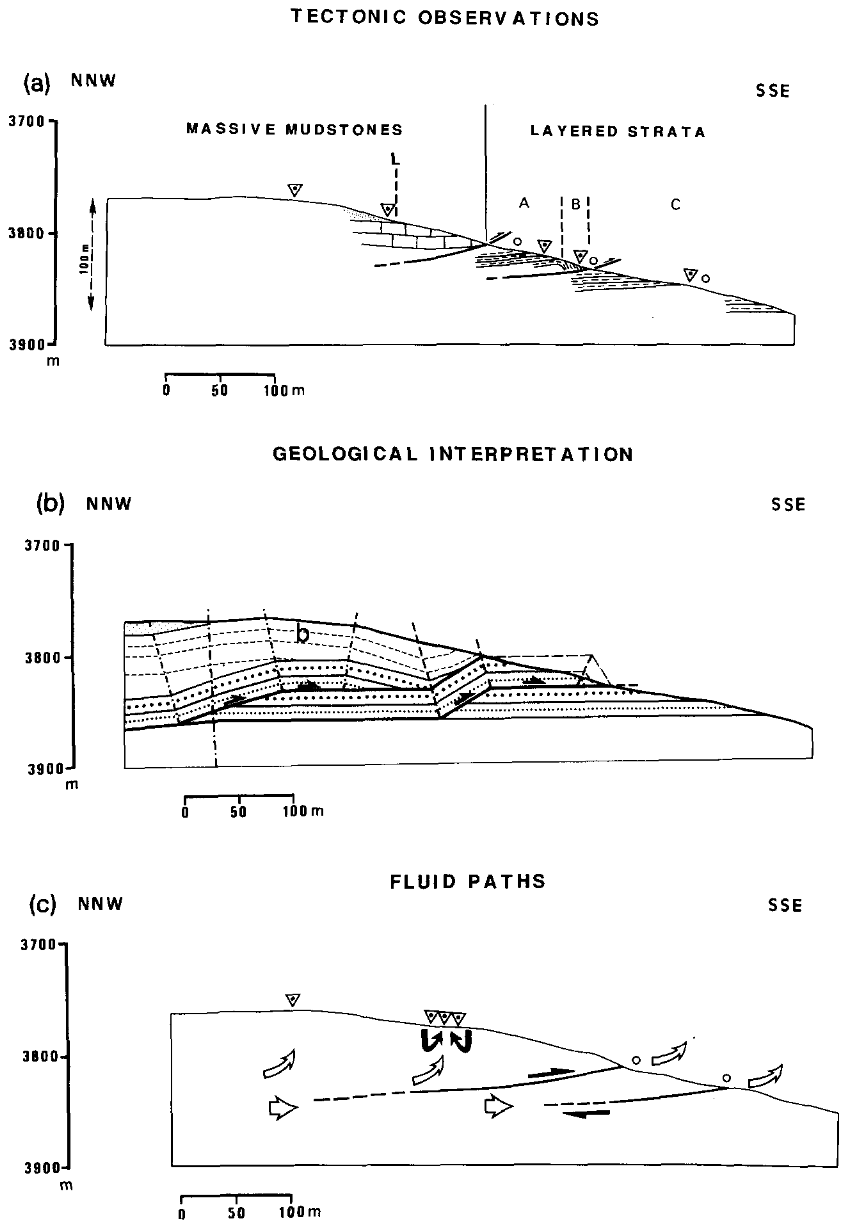

Fig. 8. Small-scale cross sections of the upslope cliff. (a) *Tectonic observations*: Triangles are clams colonies and circles are white patches. The main detachment fault between the massive mudstones and the layered strata is shown, as is a potential thrust in the layered turbidites. Zones A and C are areas of subhorizontal strata, zone B is the narrow zone of tilted strata. *L* is the limit of outcrop observed from submersible. (b) *Geological interpretation*: The geometry of the two ramp-and-flat systems was derived from the structural information obtained by submersible (see text). (c) *Possible fluid paths*: Symbols are the same as in (a). White arrows indicate circulation of undiluted fluids in the detachment fault zone. Black arrows indicate local convection beneath clam colonies.

grate along the shallow detachment fault and flow out both at the emergence of the detachment fault at the base of the cliff and above it across the overlying strata through a dense network of joints.

These results indicate that this shallow detachment fault must have a higher along-strike permeability to channel the fluids. The concentration of shallow convection between the detachment fault outcrop and the apex of the fold is probably due to higher vertical permeability there produced by the high density of joints and the absence of significant sedimentation. The absence of fluid venting and related secondary convection on the landward side of the apex may be due either to less-developed jointing or to sedimentation clogging the joints or a combination of both. In addition, the proximity of the frontal slope produces gravitational stresses which may help in developing jointing and opening existing joints. It also favours erosional slumping and scouring by currents.

Relating fluid migration along the shallow detachment fault to deeper flow along the main décollement is rather speculative. If our interpretation is correct, the upper outer unit (i.e. the shallow wedge-shaped deformed structure) is, over its entire width, mechanically decoupled from the lower sequences. Thus the shallow detachment fault is connected to the second major thrust T1b, where the inner unit thrusts over the outer unit. Evidence for fluid venting, including cylindrical chimneys and white patches, was discovered during one dive at the emergence of this thrust, suggesting that this fault is a major conduit possibly connected to the main décollement. Although we have no argument for fluid migration along the main décollement in the Nankai prism, our interpretation of the fluid path is not incompatible with such a deep origin for the fluid.

9. Conclusion

During the previous Kaiko cruise, we found that the surface trace of the eroded frontal thrust was the site of active seeps within the Tenryu Canyon [11,16]. A different situation prevails 40 km to the east, where the probable outcrop of the frontal thrust is buried below much sedimentation of talus and shows no active seep. It is reasonable to assume that the absence of seep is due to clogging of the fault outcrop by sedimentation. However, our detailed structural analysis suggests that fluid flow is still tectonically controlled, but further upslope. Fluid is channelled along a complex shallow detachment fault zone outcropping about 20–40 m below the apex of the first fold. The seeps are confined to the outward slope of the fold between the detachment fault zone and the apex. Arguments based on chemical and thermal data have been used to propose that the less-diluted fluids come along the shallow detachment fault and that more diluted fluids, produced by secondary shallow convection, seep out below the colonies on the outward slope of the fold through the dense joint network. Fluid venting is thus controlled by the active thrusting along the shallow detachment fault, the absence of sedimentation and the presence of erosion, and by increased vertical permeability due to tectonic jointing. Similar shallow detachment faults exist at the toe of the Barbados accretionary wedge [3], where they may also act as conduits for long-distance fluid migration.

Acknowledgements

This paper was written in the framework of the French-Japanese Kaiko-Nankai programme, which in France is supported by the CNRS, IFREMER and the *Ministère des Relations Extérieures* and in Japan by Monbusho. It was first presented at the "International Conference on Fluids in Subduction Zones" held in Paris in November 1990. We gratefully acknowledge the Japanese Hydrographic Department for providing us with preliminary Seabeam tracks of the diving site area. We thank H. Fujimoto who supervised the Seabeam data acquisition aboard the newly built R.V. *Hakuho Maru* and provided us with high-quality bathymetric data. During the cruise, venting sites were surveyed using the deep-towed TV system of the Japan Marine Science and Technology Centre (JAMSTEC), under the supervision of Y. Monma. A. Taira is acknowledged for inviting one of us to participate in a surface-towed sidescan sonar survey in the area. G. Moore helped with the processing of the two seismic lines NK5 and NK6 made by S.

Kuramoto at the Hawaii Institute of Geophysics. C. Müller carried out the nannofossil determination. We thank J.-P. Cadet, H. Cambray, A. Fiala-Médioni, J.T. Iiyama and S. Lallemand for fruitful discussion during the many friendly hours shared at the Haïbara shore base. The participants in the pre-site surveys and the Kaiko-Nankai survey itself wish to express their thanks to the officers, engineering crews and technicians for their invaluable cooperation during the following cruises: on the R.V. *Kaiko Daigo Maru* in August 1988, on the R.V. *Shin San Maru* in June 1989, on the R.V. *Hakuho Maru* in July 1989, and on the R.V. *Nadir* and in *Nautile*.

References

1 J.C. Moore, A. Mascle and the ODP Leg 110 Scientific Party, Tectonics and hydrogeology of the northern Barbados Ridge, results from the Ocean Drilling Program Leg 110, Geol. Soc. Am. Bull. 100, 1578–1593, 1988.

2 J.C. Moore, Tectonics and hydrogeology of accretionary prisms: role of décollement zone, J. Struct. Geol. 11, 95–106, 1989.

3 S.J. Lallemant, P. Henry, J.-P. Foucher and X. Le Pichon, Detailed structure and possible fluid paths at the toe of the Barbados accretionary wedge (ODP Leg 110 area), Geology 18, 858–861, 1990.

4 M.G. Langseth, G.K. Westbrook and M.A. Hobart, Geophysical survey of a mud volcano seaward of the Barbados accretionary complex, J. Geophys. Res. 93, 1049–1061, 1988.

5 P. Henry, X. Le Pichon, S. Lallemant, J.-P. Foucher, G.K. Westbrook and M. Hobart, Mud volcano field seaward of the Barbados accretionary complex: a deep-towed side scan sonar survey, J. Geophys. Res. 95, 8917–8930, 1990.

6 X. Le Pichon, J.-P. Foucher, J. Boulègue, P. Henry, S. Lallemant, M. Benedetti, F. Avedik and A. Mariotti, Mud volcano field seaward of the Barbados accretionary complex: a submersible survey, J. Geophys. Res. 95, 8931–8944, 1990.

7 J.C. Faugères, E. Gonthier, R. Griboulard, D. Jollivet and G. Vernette, Morphology, microphysiography and sedimentary and biology patterns of surficial deposits in the South Barbados prism: Record of recent and present active tectonics, Proc. ODP, Sci. Results 110, 111–126, 1990.

8 E. Suess, B. Carson, S.D. Ritger, J.C. Moore, M.J. Jones, L.D. Kulm and G.R. Cochrane, Biological communities at vent sites along the subduction zone off Oregon, Biol. Soc. Wash. Bull. 6, 475–484, 1985.

9 J.C. Moore, D. Orange and L.D. Kulm, Inter-relationship of fluid venting and structural evolution: Alvin observations from the frontal accretionary prism, Oregon, J. Geophys. Res. 95, 8795–8808, 1990.

10 L.D. Kulm and E. Suess, Relationship between carbonate deposits and fluid venting: Oregon accretionary prism, J. Geophys. Res. 95, 8899–8915, 1990.

11 X. Le Pichon, J.T. Iiyama, J. Boulègue, J. Charvet, M. Faure, K. Kano, S. Lallemant, H. Okada, C. Rangin, A. Taira, T. Urabe and S. Uyeda, Nankai Trough and Zenisu Ridge: a deep-sea submersible survey, Earth Planet. Sci. Lett. 83, 285–299, 1987.

12 S. Ohta and L. Laubier, Deep biological communities in the subduction zone of Japan from bottom photographs taken during "Nautile" dives in the Kaiko project, Earth Planet. Sci. Lett. 83, 329–342, 1987.

13 J. Boulègue, E.L. Benedetti, D. Dron, A. Mariotti and R. Létolle, Geochemical and biogeochemical observations on the biological communities associated with fluid venting in Nankai Trough and Japan Trench subduction zones, Earth Planet. Sci. Lett. 83, 343–355, 1987.

14 D. Dron, J. Boulègue, A. Taira and C. Rangin, Geochemistry of the Tenryu Canyon deep-sea fan biological community (Kaiko), Earth Planet. Sci. Lett. 83, 356–362, 1987.

15 J. Boulègue, J.T. Iiyama, J.-L. Charlou and J. Jedwab, Nankai Trough, Japan Trench and Kuril Trench: geochemistry of fluids sampled by the submersible Nautile, Earth Planet. Sci. Lett. 83, 363–375, 1987.

16 P. Henry, S.J. Lallemant, X. Le Pichon and S.E. Lallemand, Fluid venting along japanese trenches: tectonic context and thermal modeling, Tectonophysics 160, 277–291, 1989.

17 M.G. Langseth, G.K. Westbrook and M.A. Hobart, Contrasting geothermal regimes of the Barbados Ridge accretionary complex, J. Geophys. Res. 95, 8829–8844, 1990.

18 A.T. Fisher and M.W. Hounslow, Transient fluid flow through the toe of the Barbados accretionary complex: Constraints from ODP Leg 110 heat-flow studies and simple models, J. Geophys. Res. 95, 8845–8858, 1990.

19 J.-P. Foucher, X. Le Pichon, S. Lallemant, M.A. Hobart, P. Henry, M. Benedetti, G.K. Westbrook and M.G. Langseth, Heat-flow, tectonics and fluid circulation at the toe of the Barbados Ridge accretionary prism, J. Geophys. Res. 95, 8859–8868, 1990.

20 X. Le Pichon, P. Henry and the Kaiko-Nankai Scientific Crew, Water budgets in accretionary wedges: a comparison, Philos. Trans. R. Soc. London A335, 89–104, 1991.

21 X. Le Pichon, K. Kobayashi and Kaiko-Nankai Scientific Crew, Fluid venting activity within the eastern Nankai Trough accretionary wedge: a summary of the 1989 Kaiko-Nankai results, Earth Planet. Sci. Lett., this issue.

22 P. Henry, J.-P. Foucher et al., Interpretation of temperature measurements from the Kaiko-Nankai cruise: modeling of fluid flow in clam colonies, Earth Planet. Sci. Lett., this issue.

23 J.-P. Foucher, P. Henry, X. Le Pichon and K. Kobayashi, Time-variation of fluid expulsion velocities at the toe of the eastern Nankai accretionary complex, Earth Planet. Sci. Lett., this issue.

24 B. Carson, E. Suess and J.C. Strasser, Fluid flow and mass flux determinations at vent sites on the Cascadia margin accretionary prism, J. Geophys. Res. 95, 8891–8897, 1990.

25 X. Le Pichon, P. Henry and S. Lallemant, Water-flow in the Barbados accretionary complex, J. Geophys. Res. 95, 8945–8968, 1990.
26 K. Kobayashi, J. Ashi et al., Deep-tow survey in the Kaiko-Nankai cold seepage areas, Earth Planet. Sci. Lett., this issue.
27 S.E. Lallemand, G. Glaçon et al., Seafloor manifestations of fluid seepage at the top of a 2000-metre-deep ridge in the eastern Nankai accretionary wedge: Long-lived venting and tectonic implications, Earth Planet. Sci. Lett., this issue.
28 S.J. Lallemant, S.E. Lallemand, N. Chamot-Rooke, X. Le Pichon, J.-P. Cadet, J.T. Iiyama, H. Tokuyama, S. Kuramoto and G. Glaçon, Structural study of a major back-thrust system in the Eastern Nankai accretionary prism: results from the Kaiko-Nankai submersible survey, J. Struct. Geol., submitted.
29 H. Sakai, T. Gamo, Y. Ogawa and J. Boulègue, Stable isotopic ratios and origins of the carbonates associated with cold seepage at the eastern Nankai Trough, Earth Planet. Sci. Lett., this issue.
30 T. Gamo, H. Sakai, J. Ishibashi, K. Shitashima and J. Boulègue, Methane, ethane and total inorganic carbon in fluid samples taken during the 1989 Kaiko-Nankai project, Earth Planet. Sci. Lett., this issue.
31 J. Suppe, Geometry and kinematics of fault-bend folding, Am. J. Sci. 283, 684–721, 1983.